Journal of Nuclear Medicine, published on December 4, 2014 as doi:10.2967/jnumed.114.144014

Effects of intra-tumoral inflammatory process on ^{18}F-FDG uptake: pathologic and comparative study with ^{18}F-FAMT PET/CT in oral squamous cell carcinoma

Mai Kim[1, 2], Arifudin Achmad[2,3,4], Tetsuya Higuchi[2], Yukiko Arisaka[2], Hideaki Yokoo[5], Satoshi Yokoo[1], Yoshito Tsushima[2]

Author Affiliations:

1. Department of Stomatology and Maxillofacial Surgery, Gunma University Graduate School of Medicine. Maebashi, Gunma, Japan.
2. Department of Diagnostic Radiology and Nuclear Medicine, Gunma University Graduate School of Medicine, Maebashi, Gunma, Japan.
3. Human Resource Cultivation Center, Gunma University, Kiryu, Gunma, Japan.
4. Department of Radiology, Faculty of Medicine, Gadjah Mada University, Yogyakarta, Indonesia.
5. Department of Human Pathology, Gunma University Graduate School of Medicine.

Corresponding Author and First Author:

Name: Mai Kim

Address: Department of Stomatology and Maxillofacial Surgery, Gunma University Graduate School of Medicine; 3-39-22 Showa-machi, Maebashi, Gunma 371-8511, Japan.

Telephone Number: +81-27-220-8401, *Fax Number*: +81-27-220-8409

E-mail address: kimmu@gunma-u.ac.jp

(The first author *is currently a fourth-year PhD student*)

Word Count: 4,954

Running Title: ^{18}F-FDG & ^{18}F-FAMT in OSCC Inflammation

ABSTRACT

Accurate depiction of both biological and anatomical profile of tumor has long been a challenge in PET imaging. An inflammation, which is innate in the carcinogenesis of oral squamous cell carcinoma (OSCC), frequently complicates the image analysis due to the limitations of ^{18}F-fluorodeoxyglucose (^{18}F-FDG) and maximum SUV (SUV_{max}) unit. New PET parameters, metabolic tumor volume (MTV) and total lesion glycolysis (TLG) are considered more comprehensive in tumor image analysis, as well as ^{18}F-fluoro-α-methyltyrosine (^{18}F-FAMT), a malignancy-specific amino acid-based PET radiotracer. Here we showed the substantial effects of intra-tumoral inflammatory process on ^{18}F-FDG uptakes and further study the possibility of MTV and TLG to predict both tumor biology (proliferation activity) and anatomy (pathological tumor volume).

Methods. ^{18}F-FDG and ^{18}F-FAMT PET images from 25 OSCC patients were analyzed. SUV_{max} on the tumor site was obtained. PET volume computerized assisted reporting (PET-VCAR) was used to generate a volume of interest (VOI) to obtain MTV and TLG for ^{18}F-FDG and total lesion retention (TLR) for ^{18}F-FAMT. The whole tumor dissected from surgery were measured and sectioned for pathological analysis of tumor inflammation grade and Ki-67 labeling index (Ki-67 LI).

Results. The high SUV_{max} values of ^{18}F-FDG were related to the high inflammation grade. ^{18}F-FDG to ^{18}F-FAMT SUV_{max} ratio was higher in inflammatory tumors ($P < 0.05$) while the corresponding value in tumor with a low inflammation grade was kept low. All of ^{18}F-FAMT parameters were correlated with Ki-67 LI ($P < 0.01$). Pathological tumor volume predicted from MTV of ^{18}F-FAMT was more accurate ($R = 0.90$, bias = 3.4 ± 6.42 cm^3, 95% CI = 0.77-6.09 cm^3) than that of ^{18}F-FDG ($R = 0.77$, bias = 8.1 ± 11.17 cm^3, 95% CI = 3.45-12.67 cm^3).

Conclusions. ^{18}F-FDG uptake was overestimated by additional uptake related to intra-tumoral inflammatory process, while ^{18}F-FAMT simply accumulated in tumors according to tumor

activity as evaluated by Ki-67 LI in OSCC.

Keywords: Inflammation, MTV, OSCC, ^{18}F-FAMT, ^{18}F-FDG

INTRODUCTION

A worldwide estimation of newly diagnosed oral cavity cancer in 2008 was more than 250,000, with an estimated mortality number reached 128,000 (*1*). Ninety percent of oral cavity cancer is oral squamous cell carcinoma (OSCC) derived from mucosal lining (*2*), which is directly exposed to the external environment. Despite the advancement of diagnostic imaging and detection of biological markers, no significant improvement in survival rate was obtained over the past forty years (*3*).

OSCC PET imaging using ^{18}F-fluorodeoxyglucose (^{18}F-FDG) and maximum SUV (SUV_{max}) assessment is helpful for pretreatment staging and improved TNM classification (*4, 5*). Even though it has been considered as an independent prognostic factor (*6*), the shortcoming of semi-quantitative unit SUV_{max} is its dependency on a mere single pixel (*7*), which may not represent the whole tumor entity (*8*). Moreover, several major limitations of the SUV concept affect its reliability as a surrogate of the targeted quantity, the metabolic rate of ^{18}F-FDG (*9*).

The ^{18}F-FDG accumulation in tumor cell depends on glucose metabolism, providing a very sensitive modality for malignancy with the cost of its specificity and ability to depict the true tumor biology. To address this, amino acid based PET radiotracer ^{18}F-fluoro-α-methyltyrosine (^{18}F-FAMT) was developed, which accumulates exclusively in malignant tumor cells through the L-type amino acid transporter 1 (LAT-1) (*10-12*). In the previous OSCC studies, ^{18}F-FAMT is better than ^{18}F-FDG in its correlation with tumor proliferation activity, represented by Ki-67 labeling index (Ki-67 LI) (*13, 14*). Moreover, significant false-positive accumulation of ^{18}F-FDG in inflammatory lesions, other non-malignant lesions and in some normal organs due to physiologic activity contributes to its lower specificity for malignancy.

Recently, metabolic tumor volume (MTV) and total lesion glycolysis (TLG), which quantify both anatomical and pathophysiological aspects of the entire tumor have been introduced as new evaluation parameters in ^{18}F-FDG PET, and used as independent prognostic

biomarkers in various solid malignancies (*15-17*). The addition of these new biomarkers into American Joint Committee on Cancer stage may provide more reliable outcome prediction in oral cancer patients (*18*).

^{18}F-FAMT discriminates malignant tumors from benign lesions in oral malignancies (*14, 19*). Moreover, in OSCC, ^{18}F-FAMT provides more accurate assessment of bone marrow invasion than ^{18}F-FDG (*10*). In this study, we investigated how ^{18}F-FDG and ^{18}F-FAMT PET parameters (SUV_{max}, MTV and TLG or total lesion retention (TLR)) might be affected by intra-tumoral inflammatory process through a study with tumor inflammation grade obtained from post-surgical specimen pathological examination.

MATERIALS AND METHODS

Patients

The study involved 25 OSCC patients (11 men and 14 women aged 31–88 years; mean 61.9 years) who were referred for surgery during April 2008 to March 2013. All patients underwent surgery after ^{18}F-FDG and ^{18}F-FAMT PET/CT imaging. The study protocol was approved by the institutional review board of Gunma University and all patients agreed to participate in the study signed a written informed consent.

Radiopharmaceuticals And PET Image Analysis

^{18}F-FAMT and ^{18}F-FDG were produced in our hospital cyclotron facility. ^{18}F-FAMT was synthesized by the method developed by Tomiyoshi et al (*20*). ^{18}F-FDG or ^{18}F-FAMT were administered intravenously at a dose of 5.0 MBq/kg after fasting for at least six hours. PET study was performed 64.0 (±12.2) and 66.0 (±14.0) minutes later for ^{18}F-FDG and ^{18}F-FAMT, respectively, using a PET/CT scanner (Discovery STE, GE Healthcare) with a 700-mm field of view and slice thickness of 3.27 mm. Three-dimensional data acquisition was done for three minutes per bed position followed by the image reconstruction with 3D-OSEM method. The segmented attenuation correction was performed by X-ray CT (140 kV, 120–240 mAs) to produce 128 ×128 matrix images.

All patients underwent ^{18}F-FDG PET imaging first and then continued with ^{18}F-FAMT PET before surgery. One of three experienced nuclear medicine physicians (minimum five year experience in general nuclear medicine and four years in PET/CT) interpreted each PET images of ^{18}F-FAMT and ^{18}F-FDG. The tumors were first examined visually for abnormal ^{18}F-FDG or ^{18}F-FAMT accumulation, on where regions of interest (ROI) covering the whole tumor were placed manually over every axial image plane, to obtain SUV_{max} for a semi-quantitative analysis of tumor uptake.

PET tumor volumes were calculated using PET-VCAR, an automated segmentation software (Advantage Workstation, GE Healthcare). With a pre-determined pathologically-confirmed cutoff SUV value of 3.0 for ^{18}F-FDG and 1.4 for ^{18}F-FAMT from previous PET study of maxillofacial tumors (*19*), PET-VCAR performs auto-segmentation to the threshold-defined volumes and automatically calculates MTV and average SUV (*10*). TLG of ^{18}F-FDG was calculated by multiplying MTV with the average SUV within that volume. A similar formula was used to determine TLR of ^{18}F-FAMT. TLR is defined as a similar parameter to TLG in which describes the quantitative amount of ^{18}F-FAMT trapped in tumor cells. For semi quantitative comparison, ^{18}F-FDG-to-^{18}F-FAMT ratios of SUV_{max}, MTV and TLG/TLR were calculated.

Tumor Histopathological Analysis

The surgical specimens were fixed in 10% formalin solution, paraffin-embedded, decalcified when needed overnight and sectioned (3 μm) for pathological and immunohistochemical analysis. Pathological tumor volume (PTV) measured three-dimensionally using the length (*l*), width (*w*) and thickness (*t*) by the classical formula: (π/6) x *l* x *w* x *t*.

Haematoxylin-Eosin (H-E) staining was performed for inflammation analysis. A four-grade classification of inflammation was used based on the distribution of inflammatory cells within the tumor tissue and its surroundings (Table 1) (*21*). Tumor with inflammation grade of 2 and 3 were considered to have a severe inflammation, while grade 0 and 1 are similar to normal organs. Immunohistochemical staining was performed using the labeled streptavidin biotinylated antibody (LSAB) method (*14*). Molecular immunology borstel-1 or MIB-1 (Dako), a murine monoclonal antibody specific for human nuclear antigen Ki-67 was used in a 1:100 dilution.

Statistical Analysis

Non-parametric tests (Spearman's rank test and Mann-Whitney U test) were employed to determine the statistical difference of variables. Relationships within variables were measured using Pearson correlation analysis. For both radiotracers' MTV, further analysis using Bland-Altman analysis was used to further determine their degree of agreement with pathological tumor volumes. Probability values of < 0.05 indicated a statistically significant difference. Results were shown as means ± standard deviation (SD).

RESULTS

Patients

The average time interval from the last ^{18}F-FDG PET to ^{18}F-FAMT PET was 9.8 ±10.8 days (range: 2-56 days); and the average time interval from ^{18}F-FAMT PET studies to surgery is 16.7 days (±10.1 days). All patients' characteristics, their tumor PET quantitative values, tumor volume and Ki-67 LI were summarized in Table 2. Inflammations were found in all patients' tumor.

Inflammation Involvement In PET Images And Histological Sections

The high ^{18}F-FDG SUV_{max} without correspondingly high ^{18}F-FAMT SUV_{max} was shown on the right lower quadrant of the Pearson correlation graph in Figure 1 (R = 0.53, P = 0.003). This tendency was further described in Figure 2A, where ^{18}F-FDG-to-^{18}F-FAMT SUV_{max} ratio is significantly higher in Grade 2 and 3 group (P = 0.030), showed that high SUV_{max} of ^{18}F-FDG was significantly correlated with advanced tumor inflammation.

On the opposite, the ^{18}F-FDG-to-^{18}F-FAMT ratio of MTV and TLG-TLR showed no difference between inflammation groups (Figure 2B, P = 0.76; and Figure 2C, P = 0.10, respectively). However, some outliers were observed and suggest for more cautious interpretation.

Spearman's rank correlation coefficients showed that Ki-67 LI correlated with all of PET parameters (Table 3). Even though SUV_{max} of both radiotracers correlates with Ki-67, in ^{18}F-FAMT, a correlation coefficient of MTV and TLR were ρ = 0.718 and ρ = 0.748, while, in ^{18}F-FDG, correlation coefficients of MTV and TLG were lower ρ = 0.546 and ρ = 0.619, respectively. The SUV_{max} of ^{18}F-FDG and ^{18}F-FAMT were only moderately correlated each other (ρ = 0.578), while their MTV and TLG/TLR were strongly correlated (ρ = 0.814 and 0.873, respectively).

The potentials of MTV to predict the actual tumor volume using of both radiotracers

were evaluated by direct comparisons with PTV. MTV values of ^{18}F-FAMT and ^{18}F-FDG provided a good estimation of the actual tumor volume (Figure 3A, R = 0.77 and R = 0.90, respectively). Bland-Altman analysis (Figure 3B) further describes that tumor volumes measured by MTV of ^{18}F-FAMT is showed better agreement with actual tumor volume (bias = 3.4 ± 6.42 cm^3, 95% CI = 0.77-6.09 cm^3) than that of ^{18}F-FDG MTV (bias = 8.1 ± 11.7 cm^3, 95% CI = 3.45-12.67 cm^3).

Case Figures

A representative case presented in Figure 4 (Patient no. 20) showed that both ^{18}F-FDG and ^{18}F-FAMT SUV_{max} parameters demonstrate high uptakes. Ki-67 LI from his pathological specimen was also high (87.6%). However, H-E staining showed that inflammation in this tumor is minimal.

Discordant SUV_{max} finding between ^{18}F-FDG and ^{18}F-FAMT (Patient no. 2) was presented in Figure 5. In this case, low uptake of ^{18}F-FAMT was suggestive for low tumor activity, as confirmed by a low Ki-67 LI. However, tumor stage of this patient was advance due to the presence of neck lymph node metastasis (also confirmed by ^{18}F-FAMT uptake). H-E staining revealed that this tumor has high-grade inflammatory cell infiltration in the invasion area and consist of mainly neutrophil granulocyte.

In two above patients, all ^{18}F-FAMT parameters correspond well with Ki-67 staining and PTV. Beside patient no. 2, two other patients (No. 7 and 15) have extremely high ^{18}F-FDG SUV_{max} without evidence of appropriate PTV, and interestingly their ^{18}F-FAMT parameters matched with their tumor size and proliferation.

DISCUSSIONS

^{18}F-FDG is the most widely used PET radiotracer for malignancies (*22*). As a glucose analog, ^{18}F-FDG accumulates in the cells through GLUT-1 receptors, which is highly expressed in most malignant cells due to their high metabolic activity. However, active non-malignant pathologic processes, such as inflammation and infection, may also enhance glycolytic metabolism. Even though it has been reported that inflammatory tumors might complicate ^{18}F-FDG PET analysis, however, this concept has not been validated (*23*).

We demonstrated that SUV_{max} of ^{18}F-FDG and ^{18}F-FAMT were only moderately correlated. Given that ^{18}F-FAMT is more tumor-specific, this finding prompted us to analyze further the inflammation involvement. Significantly higher ^{18}F-FDG-to-^{18}F-FAMT SUV_{max} ratio in inflammatory tumor strongly suggested that ^{18}F-FDG SUV_{max} was largely influenced by intra-tumoral inflammatory process.

Inflammation is an integral part of the natural course of OSCC carcinogenesis. The highly diverse surfaces in the oral cavity provide a milieu for more than 750 distinct taxa of bacteria. Thus, the oral epithelium is constantly exposed to external challenges at both cellular and molecular levels. The evidence suggests that there is a link between microbial infection and OSCC (*24*).

Tumor cell proliferation rate is reported as a prognostic factor in head and neck carcinomas (*25*). In oral cavity epidermoid carcinomas, Ki-67 expression serves as an independent prognostic factor for survival (*26*). However, it is impossible to obtain comprehensive Ki-67 status due to the invasive nature of the biopsy. Thus, developing methods to evaluate cell proliferation activity from PET images would certainly be beneficial (*27, 28*). Regarding the nature of ^{18}F-FDG, such objective could only be optimally accomplished using a more malignant-specific radiotracer.

SUV_{max} of ^{18}F-FDG PET provides prognostic information in addition to American Joint

Committee on Cancer stage (*18*), and useful for tumors aggressiveness evaluation, early detection of recurrence and outcome prediction in head and neck cancers (*16, 18*). Despite its popularity and practical application, SUV_{max} is derived only from a single pixel, thus it may not represent the whole tumor entity and does not provide any information regarding tumor biology (*29, 30*). Furthermore, SUV_{max} is highly sensitive to noise and affected by the partial volume effect (*30, 31*). These phenomena appear particularly in inflammatory lesions, therefore evaluation of both biological and anatomical figure of tumor based only on SUV_{max} value only is highly susceptible from bias (*30*).

Nowadays, advanced image analysis tools and three-dimensional display techniques allowed quick and consistent volume-based assessment. Recently, new ^{18}F-FDG PET parameters (MTV and TLG) have been introduced and showed their potential as an alternative to SUV_{max} by offering more relevant tumor information while combining both metabolic activity and three-dimensional tumor volume (*15, 16*). In lung cancer, recently these parameters serve as significant prognostic factors for survival and provide better prognostic imaging biomarkers than SUV_{max} (*31*). In OSCC, TLG was suspected to be also reliable as an independent prognostic factor for recurrence and metastasis. In head and neck cancer, adding primary tumor TLG into prognostic scoring system might be useful for risk stratification (*15*). Together, ^{18}F-FDG MTV and TLG provide such potential in OSCC treated with chemoradiotherapy (*32*). Moreover, in a recent systematic review, both parameters are accurate prognostic indicators of outcome in head and neck cancer (*33*).

In this study, we evaluated the potentials of ^{18}F-FAMT and these new PET parameters for accurate depiction of both biological and anatomical figures of oral tumors. The potential of LAT-1 as a therapeutic target in oral cancer has been described long before (*34, 35*). We designed ^{18}F-FAMT as a specific PET radiotracer for LAT-1 that is overexpressed exclusively in malignant tumors (*12*) and performed several clinical trials in comparison with ^{18}F-FDG in

oral malignancies (*10, 14, 19*). Therefore, analysis of ^{18}F-FAMT and its corresponding tumor pathological characteristics is fundamental for the development of a PET imaging-based comprehensive diagnosis of tumor growth.

Previously we reported that SUV_{max} of ^{18}F-FAMT PET images showed better correlation with Ki-67 expression and clinicopathologic variables compared to that of ^{18}F-FDG in primary tumor of OSCC (*14*). Our current study elaborated this finding by introducing new parameters in the evaluation of both PET radiotracers. Consistent with the previous report, all of ^{18}F-FAMT parameters surpassed that of ^{18}F-FDG in providing better correlation with cell proliferation activity. In particular, MTV and TLR of ^{18}F-FAMT showed their potential as SUV_{max} replacement, since they have a stronger correlation with cell proliferation activity, compared with SUV_{max}. Such findings were not observed in ^{18}F-FDG, where both new parameters performed less correlation with Ki-67. This shows that ^{18}F-FAMT is superior to ^{18}F-FDG in its accuracy to predict tumor cell growth in OSCC.

Correlation between ^{18}F-FAMT's new parameters and Ki-67 in this study revealed the potential of ^{18}F-FAMT utilization for such tool. Specificity of ^{18}F-FAMT for malignant and highly proliferating tumors is shown in Figure 4 (Case no. 20), where both of the ^{18}F-FDG and ^{18}F-FAMT SUV_{max} were highly correspond to its high expression of tumor Ki-67. As shown in Figure 5 (Case no. 2), the expression of Ki-67 correlates well with ^{18}F-FAMT uptake, while ^{18}F-FDG showed a very high uptake suggestive for false positive caused by inflammation or non-specific uptake which is prone to overestimation.

If we may further hypothesize by taking account the well-established correlation between Ki-67 and patient's survival, our findings suggest that ^{18}F-FAMT and its new parameters might provide immediate predictions of patients' survival, through the estimation of tumor cell proliferation. This relationship is currently under evaluation.

This study is limited by the use of pathologically confirmed fixed SUV cut off values for

segmentation threshold, which is exclusive for OSCC. Gradient segmentation method might be superior for other tumors compared to fixed threshold method, however similar results were not observed in head and neck cancers (*18*, *36*). Finally, this was a retrospective single-center study which the results might be subject to selection bias. In general, further investigations are needed to elucidate the effects of intra-tumoral inflammatory process on ^{18}F-FDG uptake in other types of tumors.

CONCLUSION

^{18}F-FDG uptake was overestimated by additional uptake related to intra-tumoral inflammatory process, while ^{18}F-FAMT simply accumulated in tumors according to tumor activity as evaluated by Ki-67 LI.

REFERENCES

1. Jemal A, Bray F, Center MM, Ferlay J, Ward E, Forman D. Global cancer statistics. *CA Cancer J Clin.* 2011;61:69-90.
2. Cooper JS, Porter K, Mallin K, et al. National Cancer Database report on cancer of the head and neck: 10-year update. *Head Neck.* 2009;31:748-758.
3. Zini A, Czerninski R, Sgan-Cohen HD. Oral cancer over four decades: epidemiology, trends, histology, and survival by anatomical sites. *J Oral Pathol Med.* 2010;39:299-305.
4. Lonneux M, Hamoir M, Reychler H, et al. Positron emission tomography with [^{18}F]fluorodeoxyglucose improves staging and patient management in patients with head and neck squamous cell carcinoma: a multicenter prospective study. *J Clin Oncol.* 2010;28:1190-1195.
5. Senft A, de Bree R, Hoekstra OS, et al. Screening for distant metastases in head and neck cancer patients by chest CT or whole body FDG-PET: A prospective multicenter trial. *Radiother Oncol.* 2008;87:221-229.
6. Xie P, Li M, Zhao H, Sun X, Fu Z, Yu J. ^{18}F-FDG PET or PET-CT to evaluate prognosis for head and neck cancer: a meta-analysis. *J Cancer Res Clin Oncol.* 2011;137:1085-1093.
7. Burger IA, Huser DM, Burger C, von Schulthess GK, Buck A. Repeatability of FDG quantification in tumor imaging: averaged SUVs are superior to SUVmax. *Nucl Med Biol.* 2012;39:666-670.
8. Wahl RL, Jacene H, Kasamon Y, Lodge MA. From RECIST to PERCIST: Evolving Considerations for PET response criteria in solid tumors. *J Nucl Med.* 2009;50 Supp 1:122S-150S.
9. van den Hoff J, Oehme L, Schramm G, et al. The PET-derived tumor-to-blood standard uptake ratio (SUR) is superior to tumor SUV as a surrogate parameter of the metabolic rate of FDG. *EJNMMI Res.* 2013;3:77.
10. Kim M, Higuchi T, Arisaka Y, et al. Clinical significance of ^{18}F-α-methyl tyrosine PET/CT for the detection of bone marrow invasion in patients with oral squamous cell carcinoma: comparison with ^{18}F-FDG PET/CT and MRI. *Ann Nucl Med.* 2013;27:423-430.
11. Nobusawa A, Kim M, Kaira K, et al. Diagnostic usefulness of ^{18}F-FAMT PET and L-type amino acid transporter 1 (LAT1) expression in oral squamous cell carcinoma. *Eur J Nucl Med Mol Imaging.* Oct 2013;40(11):1692-1700.
12. Wiriyasermkul P, Nagamori S, Tominaga H, et al. Transport of 3-fluoro-L-α-methyl-tyrosine by tumor-upregulated L-type amino acid transporter 1: a cause of the tumor uptake in PET. *J Nucl Med.* 2012;53:1253-1261.
13. Jacob R, Welkoborsky HJ, Mann WJ, Jauch M, Amedee R. [Fluorine-18]fluorodeoxyglucose positron emission tomography, DNA ploidy and growth fraction in squamous-cell carcinomas of the head and neck. *ORL J Otorhinolaryngol Relat Spec.* 2001;63:307-313.
14. Miyashita G, Higuchi T, Oriuchi N, et al. ^{18}F-FAMT uptake correlates with tumor proliferative activity in oral squamous cell carcinoma: comparative study with ^{18}F-FDG PET and immunohistochemistry. *Ann Nucl Med.* 2010;24:579-584.
15. Abd El-Hafez YG, Moustafa HM, Khalil HF, Liao CT, Yen TC. Total lesion glycolysis: a possible new prognostic parameter in oral cavity squamous cell carcinoma. *Oral Oncol.* 2013;49:261-268.
16. Chan SC, Hsu CL, Yen TC, Ng SH, Liao CT, Wang HM. The role of ^{18}F-FDG PET/CT metabolic tumour volume in predicting survival in patients with metastatic nasopharyngeal carcinoma. *Oral Oncol.* 2013;49:71-78.
17. Quon A, Fischbein NJ, McDougall IR, et al. Clinical role of ^{18}F-FDG PET/CT in the

management of squamous cell carcinoma of the head and neck and thyroid carcinoma. *J Nucl Med.* 2007;48 Suppl 1:58S-67S.

18. Dibble EH, Alvarez AC, Truong MT, Mercier G, Cook EF, Subramaniam RM. ^{18}F-FDG metabolic tumor volume and total glycolytic activity of oral cavity and oropharyngeal squamous cell cancer: adding value to clinical staging. *J Nucl Med.* 2012;53:709-715.

19. Miyakubo M, Oriuchi N, Tsushima Y, et al. Diagnosis of maxillofacial tumor with L-3-[^{18}F]-fluoro-alpha-methyltyrosine (FMT) PET: a comparative study with FDG-PET. *Ann Nucl Med.* 2007;21:129-135.

20. Tomiyoshi K, Amed K, Muhammad S, et al. Synthesis of isomers of ^{18}F-labelled amino acid radiopharmaceutical: position 2- and 3-L-^{18}F-α-methyltyrosine using a separation and purification system. *Nucl Med Commun.* 1997;18:169-175.

21. Klintrup K, Makinen JM, Kauppila S, et al. Inflammation and prognosis in colorectal cancer. *Eur J Cancer.* 2005;41:2645-2654.

22. Kunkel M, Forster GJ, Reichert TE, et al. Detection of recurrent oral squamous cell carcinoma by [^{18}F]-2-fluorodeoxyglucose-positron emission tomography: implications for prognosis and patient management. *Cancer.* 2003;98:2257-2265.

23. Culverwell AD, Scarsbrook AF, Chowdhury FU. False-positive uptake on 2-[^{18}F]-fluoro-2-deoxy-d-glucose (FDG) positron-emission tomography/computed tomography (PET/CT) in oncological imaging. *Clin Radiol.* 2011;66:366-382.

24. Hooper SJ, Wilson MJ, Crean SJ. Exploring the link between microorganisms and oral cancer: A systematic review of the literature. *Head Neck.* 2009;31:1228-1239.

25. Thomas B, Stedman M, Davies L. Grade as a prognostic factor in oral squamous cell carcinoma: A population-based analysis of the data. *Laryngoscope.* 2014;124:688-694.

26. Motta Rda R, Zettler CG, Cambruzzi E, Jotz GP, Berni RB. Ki-67 and p53 correlation prognostic value in squamous cell carcinomas of the oral cavity and tongue. *Braz J Otorhinolaryngol.* 2009;75:544-549.

27. Kurokawa H, Zhang M, Matsumoto S, et al. The relationship of the histologic grade at the deep invasive front and the expression of Ki-67 antigen and p53 protein in oral squamous cell carcinoma. *J Oral Pathol Med.* 2005;34:602-607.

28. Myoung H, Kim MJ, Lee JH, Ok YJ, Paeng JY, Yun PY. Correlation of proliferative markers (Ki-67 and PCNA) with survival and lymph node metastasis in oral squamous cell carcinoma: a clinical and histopathological analysis of 113 patients. *Int J Oral Maxillofac Surg.* 2006;35(11):1005-1010.

29. Murphy JD, Chisholm KM, Daly ME, et al. Correlation between metabolic tumor volume and pathologic tumor volume in squamous cell carcinoma of the oral cavity. *Radiother Oncol.* 2011;101:356-361.

30. Soret M, Bacharach SL, Buvat I. Partial-volume effect in PET tumor imaging. *J Nucl Med.* 2007;48:932-945.

31. Hyun SH, Ahn HK, Kim H, et al. Volume-based assessment by ^{18}F-FDG PET/CT predicts survival in patients with stage III non-small-cell lung cancer. *Eur J Nucl Med Mol Imaging.* 2014;41:50-58.

32. Lim R, Eaton A, Lee NY, et al. ^{18}F-FDG PET/CT metabolic tumor volume and total lesion glycolysis predict outcome in oropharyngeal squamous cell carcinoma. *J Nucl Med.* 2012;53:1506-1513.

33. Pak K, Cheon GJ, Nam HY, et al. Prognostic value of metabolic tumor volume and total lesion glycolysis in head and neck cancer: A systematic review and meta-analysis. *J Nucl Med*. 2014;55:884-890.

34. Kim CH, Park KJ, Park JR, et al. The RNA interference of amino acid transporter LAT1 inhibits the growth of KB human oral cancer cells. *Anticancer Res.* 2006;26:2943-2948.

35. Kim DK, Ahn SG, Park JC, Kanai Y, Endou H, Yoon JH. Expression of L-type amino acid transporter 1 (LAT1) and 4F2 heavy chain (4F2hc) in oral squamous cell carcinoma and its precusor lesions. *Anticancer Res.* 2004;24:1671-1675.

36. Sridhar P, Mercier G, Tan J, Truong MT, Daly B, Subramaniam RM. FDG PET Metabolic Tumor Volume Segmentation and Pathologic Volume of Primary Human Solid Tumors. *AJR Am J Roentgenol.* 2014; 202:1114–1119.

Figure 1. Correlation analysis of SUV_{max} of ^{18}F-FDG and ^{18}F-FAMT.

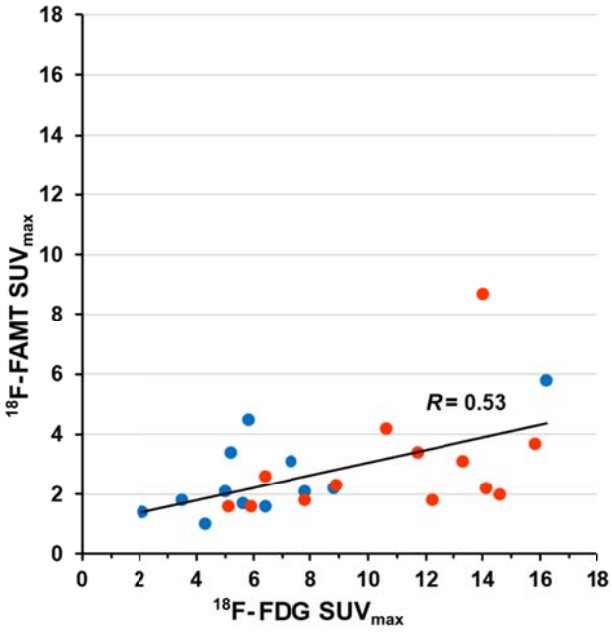

Figure 2. ^{18}F-FDG-to-^{18}F-FAMT ratio of PET parameters. ^{18}F-FDG-to-^{18}F-FAMT SUV_{max} ratio is significantly higher on tumor with high inflammation grade (A). PET metabolic parameters (MTV and TLG/TLR) showed that ^{18}F-FDG and ^{18}F-FAMT is similar when the uptake is calculated from the whole tumor (B & C).

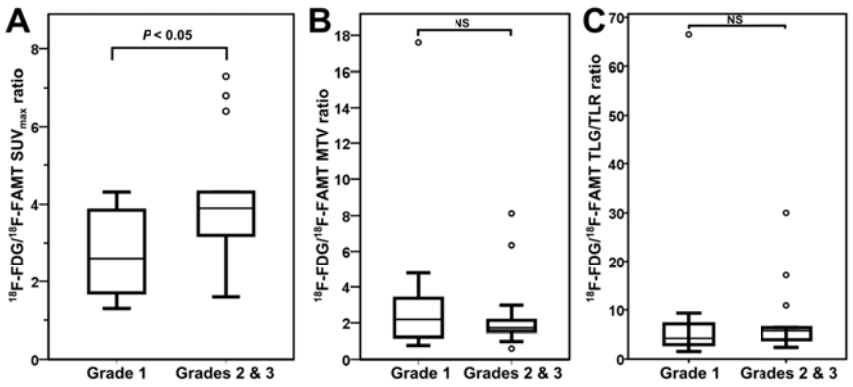

Figure 3. Prediction of actual tumor volume using MTV of ^{18}F-FDG and ^{18}F-FAMT (A). Bland-Altman analysis (B). ^{18}F-FAMT MTV predicts tumor size more accurately.

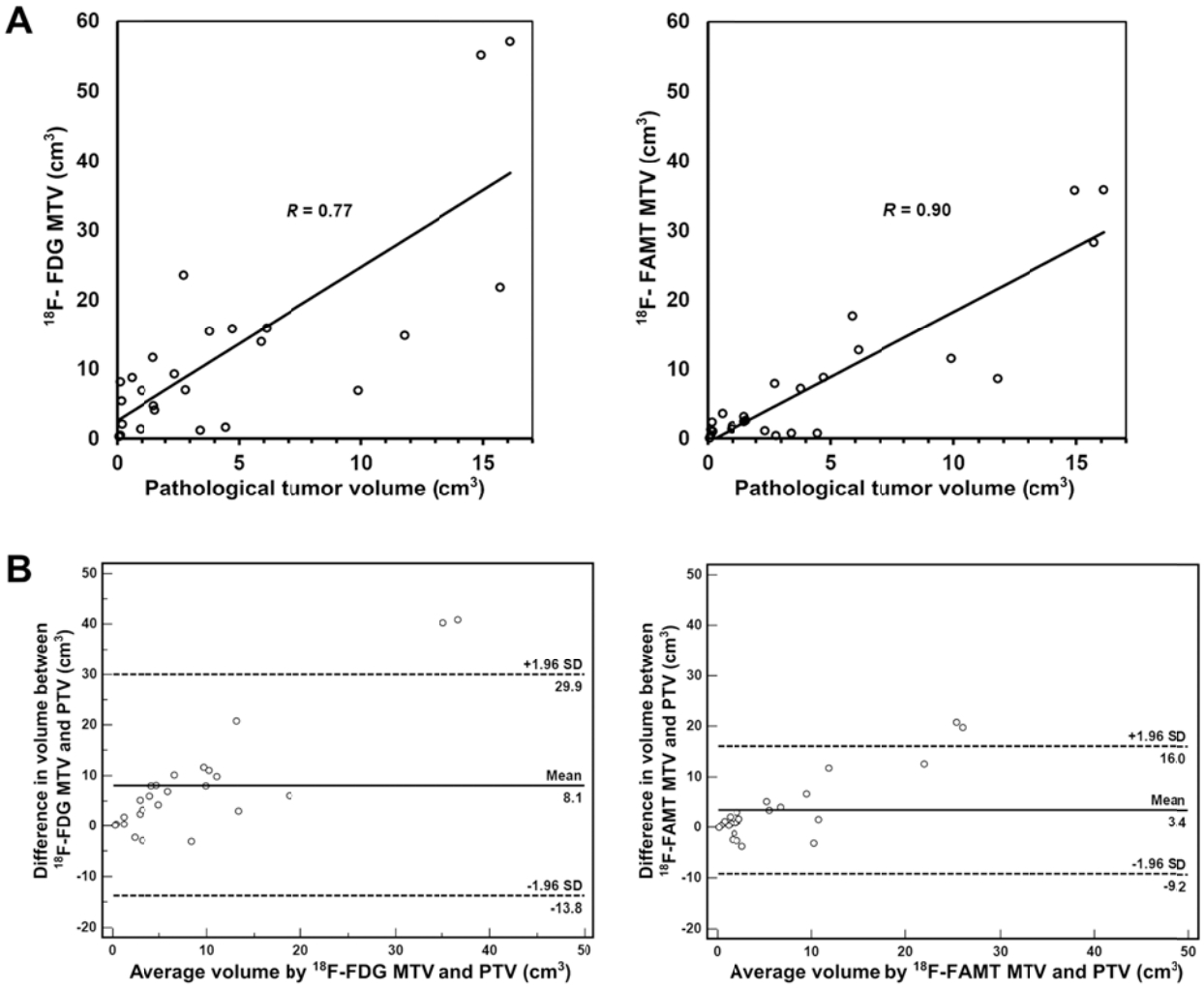

Figure 4. A 40-year-old male with OSCC in the right buccal region. Mean Intensity Projection (MIP) and coronal images of ^{18}F-FDG and ^{18}F-FAMT PET of the primary lesion (A). High ^{18}F-FDG tumor uptake was noted as well as ^{18}F-FAMT. Concordant high uptake of ^{18}F-FDG (SUV_{max} =16.2) and ^{18}F-FAMT (SUV_{max} = 5.8) were also noted. A high Ki-67 LI value (87.6%) is shown in immunohistochemistry sections (B) while H-E staining showed Grade 1 tumor inflammation (C).

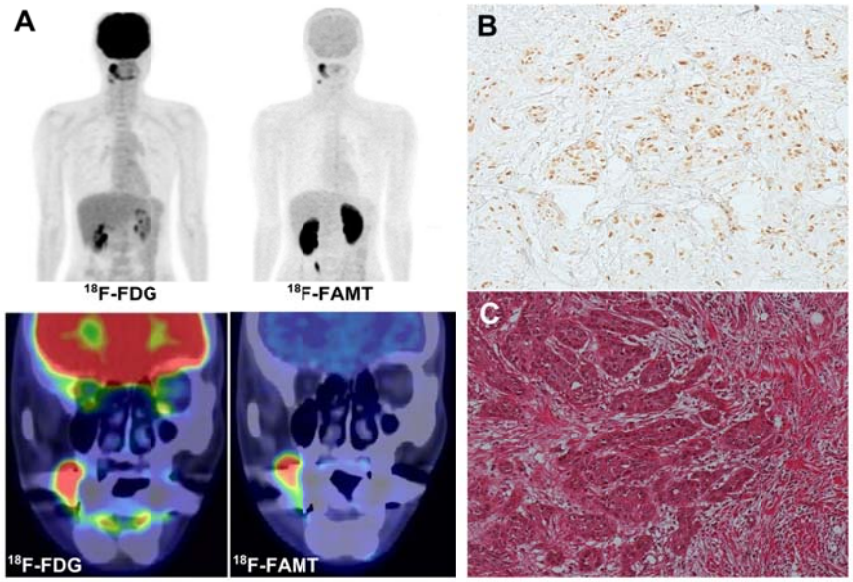

Figure 5. An 88-year-old female with OSCC in the left maxilla region. MIP and axial images of ^{18}F-FDG and ^{18}F-FAMT PET of the primary lesion (A). A high ^{18}F-FDG uptake (SUV_{max} = 12.2) is noted while on the same plane, ^{18}F-FAMT uptake (SUV_{max} = 1.8) is low. Low tumor proliferation activity is showed by low Ki-67 LI value (39.3%) (B), while H-E staining showed Grade 3 tumor inflammation (C).

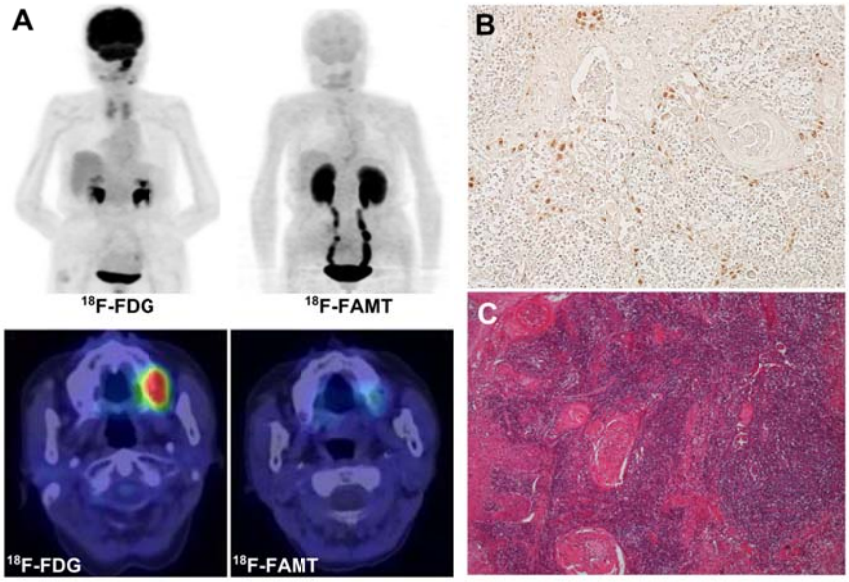

TABLE 1
Tumor Inflammation Grade

Grade	Interpretation
0	No inflammatory cells were present
1	Inflammatory cells are visible at the invasive margin, however invading cancer cell islets remain intact
2	Inflammatory cells spread within the tumor area with some destruction of invading cancer islets
3	Very prominent inflammatory reaction within the tumor with frequent destruction of cancer islets. Inflammatory cells also found beyond the

TABLE 2
Characteristic of Patients and Tumors

Patient No.	Age/ Sex	Primary tumor origin	Stage	^{18}F-FDG Parameters			^{18}F-FAMT Parameters			^{18}F-FDG to ^{18}F-FAMT			Inflammation Grade	Ki67 LI	Pathological Tumor Volume (cm^3)
				SUV_{max}	MTV	TLG	SUV_{max}	MTV	TLR	SUV_{max} ratio	MTV ratio	TLG-TLR ratio			
1	61/F	Tongue	I	5.2	8.8	28.9	3.4	3.6	7.3	1.5	2.4	4.0	1	41.7	0.6
2	88/F	Maxilla	IVa	12.2	15.8	85.4	1.8	8.8	13.2	6.8	1.8	6.5	3	39.3	4.7
3	67/M	Mandible	II	5.0	5.4	18.5	2.1	2.4	4.1	2.4	2.3	4.5	1	27.6	0.2
4	37/F	Tongue	I	5.9	4.1	14.8	1.6	2.7	3.7	3.7	1.5	4.0	2	42.4	1.6
5	59/M	Tongue	II	7.3	11.7	48.0	3.1	2.5	5.1	2.4	4.8	9.3	1	48.7	1.5
6	73/M	Tongue	I	8.8	7.0	27.9	2.2	1.9	3.2	4.0	3.7	8.8	1	40.8	1.0
7	50/M	Tongue	II	14.6	9.3	51.4	2	1.2	1.7	7.3	8.1	29.8	2	46.2	2.4
8	75/F	Tongue	I	6.4	1.4	5.6	2.6	1.4	2.3	2.5	1.0	2.4	2	44.8	0.9
9	57/M	Floor of mouth	I	7.8	4.7	19.4	2.1	3.2	5.1	3.7	1.5	3.8	1	51.3	1.5
10	61/F	Tongue	I	7.8	2.1	8.9	1.8	1.0	1.5	4.3	2.0	5.8	2	21.1	0.2
11	66/F	Tongue	IVa	5.8	21.8	80.6	4.5	28.3	50.9	1.3	0.8	1.6	1	79.3	15.7
12	51/F	Mandible	I	5.1	8.2	28.7	1.6	1.3	1.7	3.2	6.3	17.1	2	18.6	0.1
13	50/M	Mandible	III	8.9	14.9	65.6	2.3	8.6	13.8	3.9	1.7	4.7	2	62.2	11.8
14	54/M	Tongue	II	10.6	15.9	71.7	4.2	12.8	25.6	2.5	1.2	2.8	3	82.7	6.1
15	66/F	Mandible	II	14.1	23.6	139.1	2.2	7.9	12.6	6.4	3.0	11.0	3	56.8	2.7
16	78/F	Mandible	III	15.8	6.9	149.5	3.7	11.6	24.3	4.3	0.6	6.2	2	67.0	9.9
17	81/F	Floor of mouth	IVa	13.3	15.5	93.1	3.1	7.3	14.5	4.3	2.1	6.4	2	64.1	3.8
18	65/F	Maxilla	II	11.7	57.1	342.6	3.4	35.9	71.8	3.4	1.6	4.8	2	52.3	16.1
19	79/F	Tongue	II	4.3	7.0	23.9	1.0	0.4	0.4	4.3	17.6	66.5	1	14.4	2.8
20	40/M	Buccal	IVa	16.2	13.9	79.5	5.8	17.7	42.4	2.8	0.8	1.9	1	87.6	5.9
21	65/F	Tongue	II	6.4	1.7	6.6	1.6	0.8	1.2	4.0	2.1	5.5	1	65.5	4.5
22	67/M	Mandible	IVa	14.0	55.2	320.2	8.7	35.8	89.5	1.6	1.5	3.6	2	54.1	14.9
23	31/M	Tongue	I	5.6	1.2	4.6	1.7	0.8	1.0	3.3	1.5	4.8	1	30.6	3.4
24	62/M	Tongue	I	3.5	0.5	1.6	1.8	0.5	0.8	1.9	1.0	2.1	1	11.6	0.1
25	65/F	Tongue	I	2.1	0.3	0.5	1.4	0.1	0.1	1.5	3.0	4.0	1	38.3	0.1

TABLE 3

Spearman's Rank Correlation Coefficients for All PET parameters, Ki-67 and pathological tumor volume

		Ki67	^{18}F-FDG			^{18}F-FAMT			Pathological tumor volume (cm^3)
			SUV_{max}	MTV	TLG	SUV_{max}	MTV	TLR	
Ki67		1.0000							
^{18}F-FDG	SUV_{max}	0.6749*	1.0000						
	MTV	0.5462*	0.5975*	1.0000					
	TLG	0.6192*	0.7511*	0.9169*	1.0000				
^{18}F-FAMT	SUV_{max}	0.7039*	0.5783*	0.6388*	0.6935*	1.0000			
	MTV	0.7182*	0.6506*	0.8140*	0.8602*	0.8305*	1.0000		
	TLR*	0.7477*	0.6653*	0.8254*	0.8731*	0.8770*	0.9890*	1.0000	
Pathological tumor volume (cm^3)		0.7454*	0.6114*	0.6769*	0.7277*	0.5486*	0.7386*	0.7362*	1.0000

All correlations were calculated using independent data points from 25 patients.

* $P < 0.01$